ELSEVIER

Journal of Alloys and Compounds 223 (1995) 77–80

Journal of ALLOYS AND COMPOUNDS

Characteristics of the stoichiometric and non-stoichiometric Laves phase alloys and their hydride electrodes

Gao Xueping, Song Deying, Zhang Yunshi, Wang Genshi, Shen Panwen

Institute of New Energy Material Chemistry, Nankai University, TianJin 300071, People's Republic of China

Received 20 May 1994; in final form 29 September

Abstract

The pressure–composition isotherms, lattice parameters and electrode properties of the stoichiometric and non-stoichiometric C14 Laves phase alloys with various compositions were studied in this work. The flatness of the plateau pressure of the stoichiometric alloys with vanadium was inferior; however the flatness of the non-stoichiometric alloys on adding manganese improved for the $Ti_{1-x}Zr_xFe_{0.15}Mn_{0.21+y}V_{0.64}Ni_{1.0}$ ($x=0.2$–0.4, $y=0$–0.4) system. The changes in the hydrogen plateau pressure and flatness of the plateau pressure were attributed to the geometric factor and affinity of environmental elements of the tetrahedral interstices hydrogen occupation. The electrode properties of all alloys studied were dependent on the hydrogen plateau pressure and flatness of the plateau pressure of the alloy.

Keywords: Laves phase alloys; Hydride electrodes

1. Introduction

Nickel–metal hydride (Ni–MH) batteries using a hydrogen storage alloy as a negative electrode have been developed and commercialized because of their high energy density, high rate capability and cleanliness. Many kinds of hydrogen storage alloy have been examined as potential electrodes [1,2]. Recently, Laves phase metal hydrides have been studied because of their large hydrogen absorbing capacity and relatively long electrochemical charge–discharge cycles [3,4]. Among these Laves phase metal hydrides, non-stoichiometric Laves phase alloys showed excellent hydriding and electrochemical characteristics compared with stoichiometric alloys. In particular, they have the advantages of smaller slopes of the plateau for PCT curves, shorter charge–discharge cycles for activation and high electrocatalytic activities due to the second phase.

In this work, we have studied the stoichiometric and non-stoichiometric Ti–Mn-based Laves phase alloy hydrides.These alloys were found to have a C14 type Laves phase structure. By substituting A or B (AB_α $\alpha=2.0$–2.4) components, alloy hydrogen storage performance and crystallographic parameters and their electrode characteristics were examined. In addition, we also discuss the effect on alloy storage performance of the geometric factor and affinity of the element.

2. Experimental details

The $Ti_{1-x}Zr_xFe_{0.15}Mn_{0.21+y}V_{0.64}Ni_{1.0}$ ($x=0.2$–0.4, $y=0$–0.4) alloys were prepared by arc melting in an argon atmosphere. The alloy samples were turned over and remelted several times in order to homogenize them. After that, the alloys were crushed and ground mechanically to 60–120 mesh and below 300 mesh particle size without annealing.

The hydrogen storage performance of the alloys with 60–120 mesh particle size was measured by determination of the desorption pressure–composition–temperature (PCT) characteristics at 30 °C. The hydrogen storage capacity (C_{calc}) was calculated by the following equation:

$$C_{calc}=n\times 26\,800\times[(H/M)_{p1}-(H/M)_{p2}]/M_W \quad (1)$$

where n is the total number of metal atoms per formula unit of the alloy. The subscripts (p_1 and p_2) indicate hydrogen equilibrium pressure in megapascals. M_w is the molecular weight of the alloy.

Crystallographic characterization of the hydrogen storage alloys was carried out using X-ray powder diffraction analysis. The lattice constants (a and c) and unit cell volume (V) of the hydrogen storage alloy were calculated.

The alloy powder (0.60 g) with 300 mesh particle size was mixed with carbonyl nickel powder (0.15 g)

SSDI 0925-8388(94)01423-X

and polyvinyl alcohol (PVA) (0.01 g) and then loaded in a porous nickel substrate(20×20 mm^2). After that, the substrate was dried and then pressed.

The characteristics of these resulting negative electrodes were examined using a sintered nickel electrode with a large capacity as counterelectrode and an Hg/HgO (5N KOH) electrode as reference electrode.The electrodes were charged with a current density of 50 mA g^{-1} for about 10 h in an abundant electrolyte. After every charging, the current was interrupted for 15 min to open the circuit. The discharge capacity was then measured under a current density of 50 mA g^{-1} at ambient temperature and the cut-off potential for each discharge was set to be −0.740 V.

3. Results and discussion

By X-ray diffraction analysis of the $Ti_{1-x}Zr_xFe_{0.15}Mn_{0.21+y}V_{0.64}Ni_{1.0}$ ($x=0.2$–0.4, $y=0$–0.4) alloys, it was found that these alloys have mainly a hexagonal C14 type Laves phase structure irrespective of the composition. The crystallographic parameters of the hydrogen storage alloys are summarized in Table 1. It is well known that there are three different types of tetrahedral interstices (A_2B_2, AB_3 and B_4) that are available for hydrogen occupancy in both the C14 and C15 type Laves phase structures. It has been demonstrated that the A_2B_2 tetrahedral interstices should be occupied preferentially by hydrogen because they have the largest tetrahedral holes [5]. Therefore the corresponding hard sphere radii of the A_2B_2 interstitial sites in the C14 type Laves phase structure from calculated a-axis lattice parameters are also summarized in Table 1 ($R_s=0.074475$ Å [6]). This result reveals that the lattice volume and R_s in the stoichiometric alloys ($y=0$) increased as the amount of substituted zirconium increased, but these values in the non-stoichiometric alloys ($x=0.4$) decreased when the manganese was added. In the case of the non-stoichiometric alloys, the excess manganese or vanadium atoms with larger atomic radius compared with other B atoms in AB_α intermetallic compounds substitute titanium or zirconium atoms. This substitution of elements gives rise to a decrease of the average atomic radius of A atoms in AB_α intermetallic compounds, and therefore both lattice volume and R_s decreased for the non-stoichiometric alloys. At the same time, the substitution of elements leads to a deviation from the ideal c/a ratio and a decrease in symmetry.

Table 1
Structure parameters of the $Ti_{1-x}Zr_xFe_{0.15}Mn_{0.21+y}V_{0.64}Ni_{1.0}$ ($x=0.2$–0.4, $y=0$–0.4) alloys

Alloy	Lattice parameters (Å)		Lattice volume (Å³)	c/a [a]	R_s [b] (Å)
	a	c			
$x=0.2$; $y=0$	4.905	7.994	168.58	1.630	0.3653
$x=0.3$; $y=0$	4.916	8.001	167.43	1.628	0.3661
$x=0.4$; $y=0$	4.931	8.025	169.01	1.627	0.3672
$x=0.4$; $y=0.2$	4.915	8.003	167.43	1.628	0.3660
$x=0.4$; $y=0.4$	4.903	7.993	166.42	1.630	0.3652

[a] Ideal value of $c/a=(8/3)^{1/2}=1.633$.

[b] R_s is the hard sphere radius of the A_2B_2 tetrahedral interstice in the C14 Laves phase.

The experimentally determined pressure–composition desorption isotherms for the $Ti_{1-x}Zr_xFe_{0.15}Mn_{0.21+y}V_{0.64}Ni_{1.0}$ ($x=0.2$–0.4, $y=0$–0.4) alloys at 30 °C are illustrated in Figs. 1 and 2. It is obvious that the hydrogen plateau pressure decreases and the hydrogen storage capacity (H/M at 5.1 MPa) increases as the amount of substituted zirconium increases for the stoichiometric alloys ($y=0$). This was attributed to lattice expansion and change of chemical affinity for hydrogen of the metals (zirconium has a higher chemical affinity for hydrogen than titanium does; see Table 2). These alloys are inferior in the flatness of the plateau pressure.

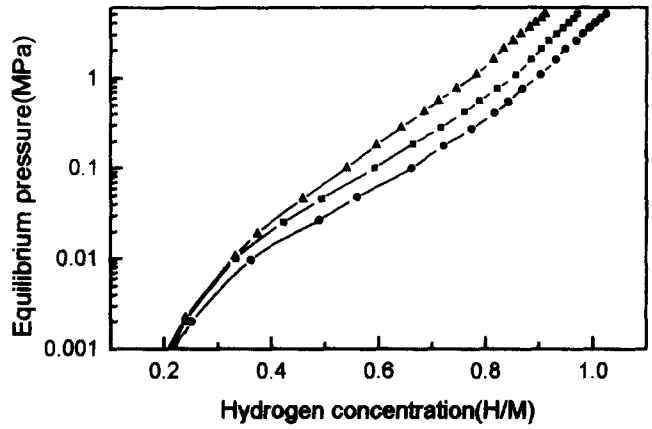

Fig. 1. PCT curves of deposition for the $Ti_{1-x}Zr_xFe_{0.15}Mn_{0.21+y}V_{0.64}Ni_{1.0}$ alloys at 30 °C: ●, $x=0.4$; ■, $x=0.3$; ▲, $x=0.2$.

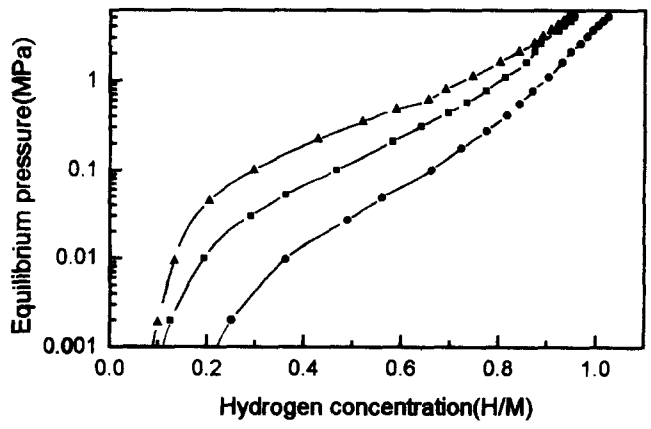

Fig. 2. PCT curves of deposition for the $Ti_{0.6}Zr_{0.4}Fe_{0.15}Mn_{0.21+y}V_{0.64}Ni_{1.0}$ alloys at 30 °C: ●, $y=0$; ■, $y=0.2$; ▲, $y=0.4$.

Table 2
Atomic radius of metals and heat of formation of metal hydrides [7–10]

Metal	Atomic radius in metal (Å)	Heat of formation of hydride (kJ mol. H^{-1})
Zr	1.60	−82 calor (ZrH_2)
Ti(α)	1.488	−68 calor (TiH_2)
V	1.321	−36 ($VH_{0.5}$)
Mn(γ)	1.366	−8 ($MnH_{0.5}$)
Fe(γ)	1.289	+10 ($FeH_{0.5}$)
Ni	1.246	−3 ($NiH_{0.5}$)

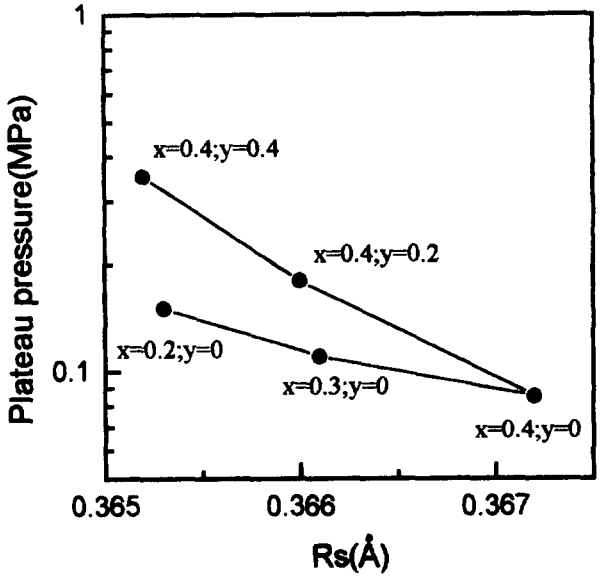

Fig. 3. The relationship between R_s and the plateau pressure for the $Ti_{1-x}Zr_xFe_{0.15}Mn_{0.21+y}V_{0.64}Ni_{1.0}$ alloys.

It is considered that the presence of vanadium has a considerable effect on the formation of solid solution of hydrogen in alloys. The nickel also has influence on the slope of the plateau pressure. In the case of the non-stoichiometric alloys ($x=0.4$), the hydrogen plateau pressure tended to increase and the hydrogen storage capacity (H/M) decreased with adding manganese, i.e. with decreasing R_s. Importantly, the flatness of the plateau pressure was improved and the residual hydrogen content was decreased. Therefore, the effect of the change of the A_2B_2 tetrahedral hole on the hydrogen storage performance is clear and is in agreement with the geometric model for the stoichiometric and non-stoichiometric alloys.

By comparison between the hard sphere radii of A_2B_2 interstitial sites of the stoichiometric and non-stoichiometric alloys (see Fig. 3), it was found that these alloys are dramatically different in the hydrogen storage performance of PCT curves, especially in both the hydrogen plateau pressure and the flatness of the plateau pressure, even if these R_s were equal or similar, such as $R_s=0.3660$ or $R_s=0.3652$ Å. Thus it is considered that these differences in hydrogen storage performance are attributed to the different chemical environment of A_2B_2 tetrahedral interstices in the above alloys. Consequently, the affinity of elements which make up the A_2B_2 tetrahedral constituents contributes to the hydriding properties of the alloys, in addition to the geometric factor.

The variation in discharge capacity of the $Ti_{1-x}Zr_xFe_{0.15}Mn_{0.21+y}V_{0.64}Ni_{1.0}$ ($x=0.2$–0.4, $y=0$–0.4) alloy electrodes with the cycle number is shown in Fig. 4. The discharge capacity was lower at the initial stage of charge and discharge and then increased gradually with increasing cycle number for all electrodes studied. These electrodes were activated fully after about 12 cycles. In the case of stoichiometric alloys ($y=0$), the electrodes became harder to activate when the amount of zirconium was increased and this result was in agreement with a previous report on the activation behaviour of zirconium-based metal hydride electrodes [3]. However, the non-stoichiometric alloy electrodes with increasing manganese were easier to activate on account of larger average electron density (e/a) of the non-stoichiometric alloy than that of the stoichiometric alloy and easier activation of the manganese. It was found that no second phase contributes to the activation for the non-stoichiometric alloy electrodes.

The discharge capacity and calculated electrochemical capacity of the mentioned above negative electrodes are given in Table 3. For the Laves phase alloy the calculated electrochemical capacity from PCT data is somewhat different from that of Mm–Ni-based hydrogen storage alloy because of the inferior flatness of the plateau pressure due to hydrogen solid solution in alloy with vanadium. Therefore the subscripts in Eq. (1) should be taken as 0.8 and 0.001, according to Nernst's

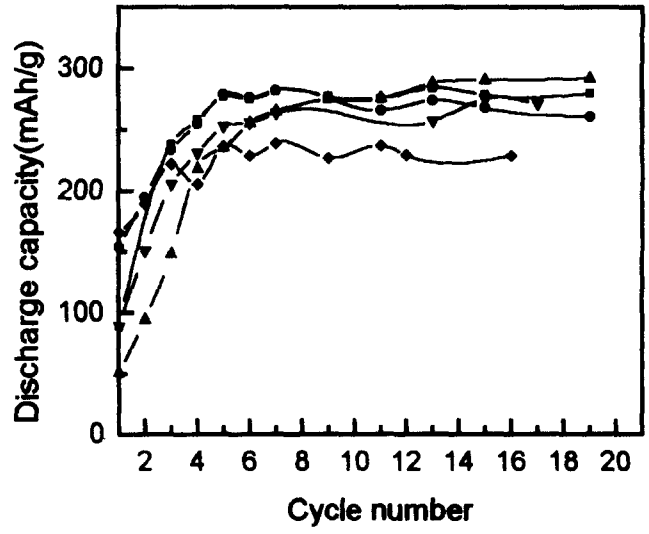

Fig. 4. Discharge capacity vs. cycle number for the $Ti_{1-x}Zr_xFe_{0.15}Mn_{0.21+y}V_{0.64}Ni_{1.0}$ alloy electrodes at a current density of 50 mA g^{-1} and an ambient temperature: ●, $x=0.2$, $y=0$; ■, $x=0.3$, $y=0$; ▲, $x=0.3$, $y=0$; ▼, $x=0.4$, $y=0.2$; ◆, $x=0.4$, $y=0.4$.

Table 3
The discharge characteristics of the $Ti_{1-x}Zr_xFe_{0.15}Mn_{0.21+y}V_{0.64}Ni_{1.0}$ ($x=0.2$–0.4, $y=0$–0.4) alloy electrodes

Alloy	$C_{max(0.2C)}$ (mAh g^{-1})	$C_{(1C)}/C_{(0.2C)}$ (%)	$C_{(0.5C)}/C_{(0.2C)}$ (%)	C_{calc} (mAh g^{-1})
$x=0.2$; $y=0$	281	71.2	87.7	283
$x=0.3$; $y=0$	284	46.4	81.9	286
$x=0.4$; $y=0$	291	35.9	76.9	295
$x=0.4$; $y=0.2$	275	45.0	81.0	290
$x=0.4$; $y=0.4$	239	73.3	91.4	274

$C_{max(0.2C)}$: maximum of discharge capacity under a discharge rate of 0.2C.

C_{calc}: the calculated hydrogen storage capacity from PCT data ($p_1=0.8$, $p_2=0.001$).

equation, respectively [11]. The changes in actual discharge capacity were correlated with the changes in calculated electrochemical capacity.

The high rate dischargeability, which is defined as $C_{(1C)}/C_{(0.2C)}$ or $C_{(0.5C)}/C_{(0.2C)}$, showed some differences, as can be seen from Table 3. In general, the high rate dischargeability is controlled by many factors such as the surface electrocatalytic activity and hydrogen diffusion in alloy and so on. On the other hand, the hydrogen plateau pressure and flatness of the plateau pressure in PCT curves also contribute to the high rate dischargeability in our investigated Laves phase alloy electrodes.

4. Conclusions

For the C14 type Laves phase stoichiometric and non-stoichiometric alloys represented as $Ti_{1-x}Zr_x$-$Fe_{0.15}Mn_{0.21+y}V_{0.64}Ni_{1.0}$ ($x=0.2$–0.4, $y=0$–0.4), the hydrogen storage performance and electrode characteristics were performed. It was found that the geometric factor and chemical affinity of environmental elements of the tetrahedral interstices for hydrogen occupation contribute to the hydrogen plateau pressure and flatness of the plateau pressure. The chemical affinity of environmental elements of the tetrahedral interstices clearly affects the hydrogen storage performance if the geometric factor remains constant. The discharge characteristics of the resulting electrodes were dependent on the hydrogen plateau pressure and flatness of the plateau pressure. The effect of substituting elements on the electrode performance was performed by changing the hydrogen storage performance of alloys.

Acknowledgments

This work was supported by the National Advanced Material Committee of China (NAMCC).

References

[1] J.J. Willems and K.H.J. Buschow, *J. Less-Common Met., 129* (1987) 13.
[2] M.A. Fetcenko, S. Venkatesan, K.C. Hong and B. Beichman, *Power Sources, 12* (1989) 411.
[3] Y. Moriwaki, T. Gamo, H. Seri and T. Iwaki, *J. Less-Common Met., 172–174* (1991) 1211.
[4] S.R. Kim and J.Y. Lee, *J. Alloys Comp., 185* (1992) L1.
[5] D.P. Shoemaker and C.B. Shoemaker, *J. Less-Common Met., 68* (1979) 43.
[6] J.R. Johnson, *J. Less-Common Met., 73* (1980) 345.
[7] J.A. Dean (ed.), *Lange's Handbook of Chemistry*, 13th edn, McGraw-Hill, New York, 1985.
[8] W.M. Mueller, J.P. Blackledge and G.G. Libowitz, *Metal Hydrides*, Academic Press, New York, 1968.
[9] H. Wenzl, *Int. Met. Rew., 27* (1982) 140.
[10] A. Driessen, H. Hemmes and R. Griessen, *Z. Phys. Chem., NF143* (1985) 145.
[11] C. Iwakura, T. Asaoka, H. Yoneyama, T. Sakai, K. Oguro and H. Ishikawa, *Chem. Soc. Jpn., 8* (1988) 1482.